Polymer 52 (2011) 752–759

Contents lists available at ScienceDirect

Polymer

journal homepage: www.elsevier.com/locate/polymer

Thermal and mechanical properties of microcellular thermoplastic SBS/PS/SBR blend: effect of crosslinking

Ruey-Sheng Shih [a,b], Shiao-Wei Kuo [c], Feng-Chih Chang [b,*]

[a] Microcell Composite Company, Tainan 717, Taiwan
[b] Institute of Applied Chemistry, National Chiao Tung University, Hsinchu 300, Taiwan
[c] Department of Materials and Optoelectronic Science, Center for Nanoscience and Nanotechnology, National Sun Yat-Sen University, Kaohsiung 804, Taiwan

ARTICLE INFO

Article history:
Received 29 June 2010
Received in revised form
30 November 2010
Accepted 14 December 2010
Available online 21 December 2010

Keywords:
SBS
SBR
Crosslinking

ABSTRACT

This study investigates the effect of peroxide crosslinking on the structure and mechanical properties for SBS/PS/SBR foams composed of polystyrene (PS), poly(styrene-*b*-butadiene) diblock copolymer (SBR-1502), and poly(styrene-*b*-butadiene-*b*-styrene) triblock copolymer (SBS). The cell size and its distribution of SBS/PS/SBR foams were investigated by SEM images, showing the smaller and denser of hollow cells for the SBS/PS/SBR foam containing the higher concentration of DCP (dicumyl peroxide). As expected, the density of the SBS/PS/SBR foams increases with increasing the content of DCP. The high density of polymeric foams exhibits the high mechanical properties such as hardness, shrinkage, tensile strength, tear strength, elongation at break, and compression set.

1. Introduction

Synthetic foams are composite materials prepared by filling a metal, polymer or ceramic matrix with hollow particles named microballoons or cells [1]. Foam polymers are two-phase gas–solid materials in which the solid polymer is continuous and gaseous cells are dispersed throughout the macromolecular support. They are important items in the economy because of technical, commercial and environmental issues; they represent an interesting dynamic in the twenty-first century society. These foams with hollow particles dispersed in the network matrix meet the need of practical commodities such as light weight, high toughness, excellent elasticity, and good resistance to thermal conductivity and acoustic reflection. With these unique properties, synthetic foams are widely applied in aircraft insulator, automotive parts, buildings fillers, packaging materials, electrical and household goods and so on. For example, refrigerator doors are filled with polyurethane (PU) foams to maintain the interior temperature for reduction in electricity consumption and sport shoes are assembled with poly(styrene-*b*-butadiene-*b*-styrene) (SBS) foams as shoe soles to cushion (shock absorption) in order to protect the heel from impact forces and enhance the athlete's performance [2]. Noticeably, polymer-supported foams account for a large number of application markets because of low-cost raw materials and easy processing of shape [3].

PU became important in the late 60s despite a complex fabrication process because they provided lower weight, greater comfort, and higher rebound resilience (elastic recovery). Thermoplastic rubbers (TPR) based on oil extended SBS were introduced in the 70s. They could be fabricated into shoe soles more easily than rubber with only minimal loss in performance. SBS is a synthetic rubber copolymer consisting of three segments of two polystyrene (PS) and one polybutadiene (PB). Due to the thermodynamic disfavor between two distinct compositions, the PS segments would self-assemble into separate microphases of PS aggregation in the PB matrix by distributing covalent bonds between PS and PB segments on the boundary of microdomains [4]. The confinement of two end groups of a PB chain on the surface of the PS hard domains can not only retard its deformation (a disentanglement process) under an external stress but also help to revert to its original size (an entanglement process) when the external stress is removed, showing the elasticity of an SBS rubber. This elastic property is very important for SBS foams because the growth of hollow gas cells in the SBS body can be restricted within a confined space (close cells) by the extended SBS networks when gas is released from the blowing agents. As well as physical additives such as CO_2, the blowing agents can be chemical additives such as azodicarbonamide (AC), decomposing to N_2, CO, and CO_2 at high temperatures (>120 °C). The latter is more expansive but has

* Corresponding author. Tel./fax: +886 3 5131512.
E-mail address: changfc@mail.nctu.edu.tw (F.-C. Chang).

0032-3861/$ – see front matter © 2010 Elsevier Ltd. All rights reserved.
doi:10.1016/j.polymer.2010.12.026

a brilliant performance on "a micellular closed foam" with the diameter of isolated cells smaller than 10 μm, probably due to the uniformly release of gas by controlling reaction temperatures [5]. Therefore, the addition of chemical blowing agents dominates the density of an SBS foam, playing an important role on the mechanical properties. However, the gas in close cells sometimes dissipates under frequent impact resulting in a so-called fatigue behavior, the progressive and localized structural damage that occurs when SBS foam is subjected to cycling loading due to the packing of polymer chains are not as dense as metals or glass, especially for those with low glass transition temperatures such as PB. This is the reason why a small number of crosslinking agents such as dicumyl peroxide (DCP) in this study are added to the SBS foams for the improvement of mechanical properties [6]. Prior to the blowing agent AC, the relatively labile DCP with the half-life temperature in dodecane at 117 °C for 10 h would decompose to two cumyloxyl radicals initiating the vinyl crosslinking reaction of PB domains [7].

In this study, we prepared six SBS foams with different densities by adjusting the compositions of AC and DCP, listed in Table 1. Instead of synthesizing new SBS copolymers with different compositions, the SBS copolymer containing 40 wt % PS was modified by blending with PS homopolymer and poly(styrene-*b*-butadiene) (SBR) diblock copolymer containing 23.5 wt % PS [8]. PS homopolymer was used to expand the size of PS domains and SBR copolymers can connect PS domains with these PB chains bearing a free end groups, making PB domains more flexible [9,10a,8a,8b]. Besides, the silicon dioxide (SiO_2) nanoparticles are also important trace additives for the heterogeneous growth of separated microballoons from these fine particles [11]. $CaCO_3$ is one of the inorganic additives that are widely used for plastics. We can make low priced and strong plastics by adding $CaCO_3$. Others such as pentaerythritol tertkis(3,5-di-*tert*-butyl-4-hydroxyhydrocinnamte) (PT) and white oil are used as antioxidant and processing oil. To give the homogeneous size distributions of gas cells from the inside out, the pressure loading between two hot plates, i.e., a compression mold coupled with a temperature control, is employed to control the expansion of gas cell [12]. The mechanical response of polymer foams depends on their architecture, and on the intrinsic properties of the materials in the cell wall [3b,3c]. Herein, the morphologies of microstructures such as the cell wall thickness, the size distribution and the shape of the cells are characterized by scanning electron microscopy (SEM). Thermal properties such as thermal stability can be measured by thermal gravity analyzer (TGA). In addition, dynamic mechanical properties such as elastic or loss modulus were characterized by dynamic mechanical analyzer (DMA) with a compression mode. Other properties are listed and discussed, including density, hardness, shrinkage, tensile strength, tear strength, elongation and compression set.

2. Experimental

2.1. Materials

Poly(styrene-*b*-butadiene-*b*-styrene) (SBS, KIBITON TPE PB-575, 33 wt % of oil content), polystyrene (PS, PS-336T), and poly(styrene-butadiene) copolymer (SBR-1502) are purchased from Chi Mei, En Chuan Chemical Industries, and TSRC Co., Ltd. in Taiwan, respectively. Pentaerythritol tetrakis(3,5-di-*tert*-butyl-4-hydroxyhydrocinnamate) (PT, 1010), silicon oxide (SiO_2, H-255 LD), white oil (WO, PW-150) are purchased from Sumitomo Chemical, PPG Industries, and Ever Light Ban Hon Co., Ltd., respectively. Azodicarbonamide (AC) and dicumyl peroxide (DCP) are purchased from Chemical Co., Ltd.

2.2. Preparation

The most significant mechanical property of an SBS foam is cushioning because the gas in the close cells can be compressed so as to absorb a shock from a transient impact and meanwhile, the extended SBS networks can get relaxed (Scheme 1) [13]. After the stress is released, the gas would dilated and then, be restricted within the extended SBS networks. The method of fabrication of SBS/PS/SBR foam samples involves five stages: (i) blending all compositions in a kneader and a two-roll mill at 120 °C according to the weight ratios listed in Table 1, (ii) making a sheet through a two-roll device, (iii) cutting it into pieces with a proper size, (iv) stacking a compression mold with a given quantity of them, (v) foaming under pressure of 120 kg/cm^2 at 160 °C for 20 min.

2.3. Characterization

A TA Instruments thermogravimetric analyzer, operated at a scan rate of 20 °C/min over temperatures ranging from 30 to 800 °C under a N_2 purge of 40 mL/min, was used to record TGA thermograms of samples on a Pt holder. Herein, sample is sandwiched between a flexed plate and a plate mounted on the drive shaft and compression stress is applied by the motor. The cylindrical compressive specimens were cut to diameter of 8.0 ± 0.05 mm and thickness of 2.5 ± 0.05 mm, and the rectangular tensile

Table 1
Compositions of SBS/PS/SBR polymer foam.

Samples	Compositions by phr[a]										
	Resins				Additives						
	SBS[b]	PS[c]	SBR-1502[d]	Total	PT[e]	SiO_2[f]	WO[g]	AC[h]	DCP[i]	$CaCO_3$	Total
I	86.4	8	5.6	100	0.3	1.3	3.2	4.66	0	36	45.46
II	86.4	8	5.6	100	0.3	1.3	3.2	4.66	0.1	36	45.56
III	86.4	8	5.6	100	0.3	1.3	3.2	4.66	0.12	36	45.58
IV	86.4	8	5.6	100	0.3	1.3	3.2	4.66	0.15	36	45.61
V	86.4	8	5.6	100	0.3	1.3	3.2	4.66	0.18	36	45.64
VI	86.4	8	5.6	100	0.3	1.3	3.2	4.66	0.2	36	45.66

[a] Parts per hundreds of resins (by weights).
[b] Poly(styrene-butadiene-styrene) triblock copolymer containing 40 wt % polystyrene block.
[c] Polystyrene.
[d] Poly(styrene-butadiene) diblock copolymer containing 23.5 wt % polystyrene block.
[e] Pentaerythritol tetrakis(3,5-di-*tert*-butyl-4-hydroxyhydrocinnamate).
[f] Silicon oxide.
[g] White oil.
[h] Azodicarbonamide.
[i] Dicumyl peroxide.

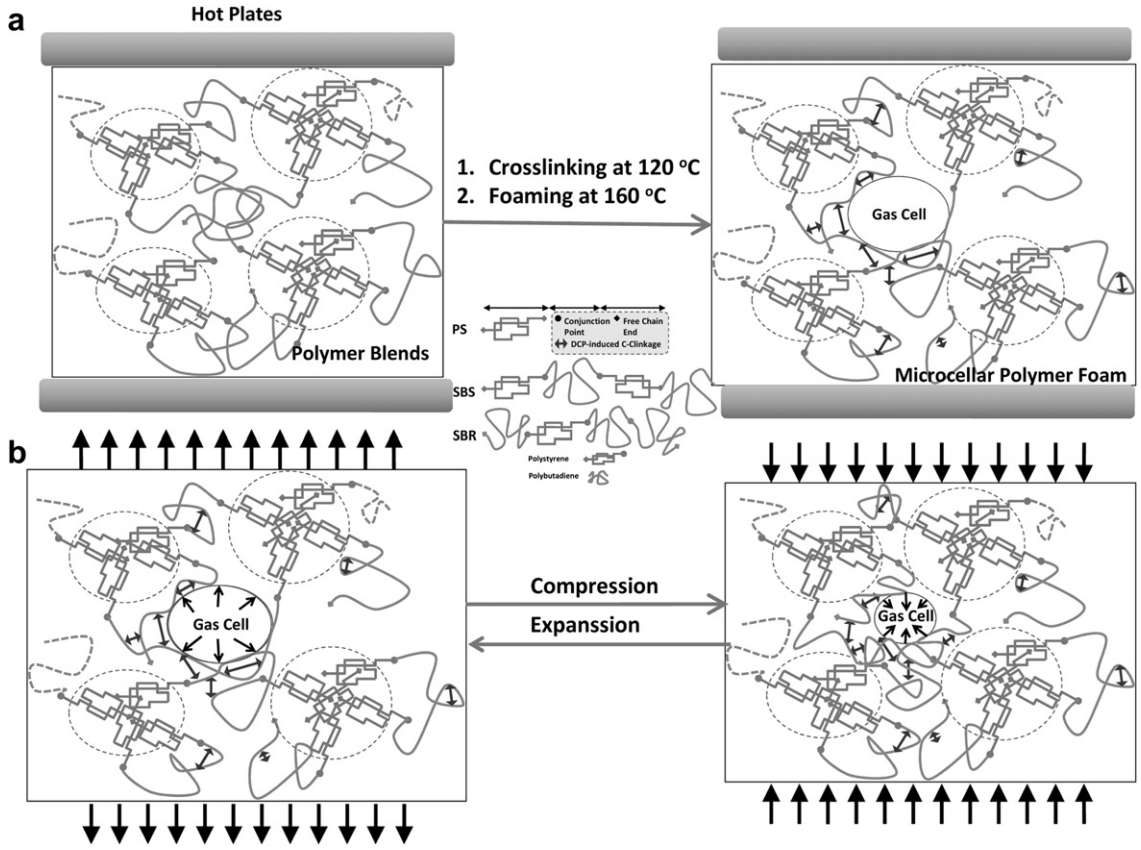

Scheme 1. (a) Compression molding and (b) elastic mechanism of SBS/PS/SBR polymer foam.

specimens were cut to length of 10.40 ± 0.05 mm, width of 7.12 ± 0.05 mm and thickness of 0.64 ± 0.05 mm. The PS/PB foams were fractured in liquid nitrogen and their surface and interface morphologies were examined using a Hitachi S-4800 FESEM. TEM images were taken for the samples with the butadiene segment stained with OsO_4, using a Hitachi H-7500 transmission electron microscope operated at an accelerating voltage of 100 kV. Ultrathin sections of the TEM samples (ca. 70 nm thickness) were prepared using a Leica Ultracut UCT microtome equipped with a diamond knife. Compression molding process is used to manufacture foam blocks of high thickness. This foaming process starts with the production of a solid sheet with the above mentioned components. A solid sheet is obtained from the previous mixture. In a first processing stage, the sheet is introduced into a mold which is closed under high-pressure (>200 bar). The mold is then heated at 160 °C in achieving suitable exotherm for further crosslinking reactions (decomposition of DCP). Simultaneously, the foaming reaction (decomposition of AC) also begins generating the gas for expansion. Finally, the samples were cut for morphological and mechanical testing. Mechanical properties for polymer foams were tested by following ASTM, including hardness, density, shrinkage, strength, elongation and compression set. Asker C hardness is measured with an Asker C durometer five times and averaged. The lower the Asker C number the softer or more compressive the foam. Compression set (CS) is measured by a modified ASTM D-395, Method B. The compression set test measures permanent set of the foam, the lower the permanent set the better the elastic recovery of the foam. Compression set was measured on three 1 in. × 1 in. × 0.5 in. foam pieces and averaged. The compression set was done at two different conditions. The first condition, which will be known at the 50 °C compression set, compressed the foam cubes by 50% for 6 h at 50 °C and then removed the compression, and the foam was allowed to recover for 30 min at room temperature. The final sample thickness was measured, and the permanent set was calculated using the following equation (1), where T_0 is the original sample thickness; T_f^{50} is the final sample thickness; and T_s is the spacer thickness. A foam sample is marked and measured for length and width. It is then put into an oven at 70 °C for 1 h at which time it is removed from the oven and allowed to cool (usually 1–4 h). Once cooled the length and width are measured, and the percentage shrinkage is calculated by the following equation (2), where T_0 is the original sample thickness and T_f^{70} is the final sample thickness.

$$CS(\%) = [(T_0 - T_f^{50})/(T_0 - T)] \times 100\% \quad (1)$$

$$Shrinkage(\%) = [(T_0 - T_f^{70})/T_0] \times 100\% \quad (2)$$

3. Results and discussion

3.1. Design of formula and process

The morphology of PS/PB microstructure after melt processing is shown in Fig. 1. As shown in Table 1, the resin with 44 wt % PS is composed of 86.4 wt % of SBS, 8.0 wt % of PS, and 5.6 wt % of SBR. After OsO_4 staining, the PB microdomains are dark, and the PS microdomains appear light. The morphological observation demonstrates that the star-block copolymer of TPE PB-575, the SBS film containing 40 wt % PS self-assembles to form worm-like PS separate phase in the PB continuous phase lacking long-range order in Fig. 1a. For the SBS/PS blends, the regularly swelling

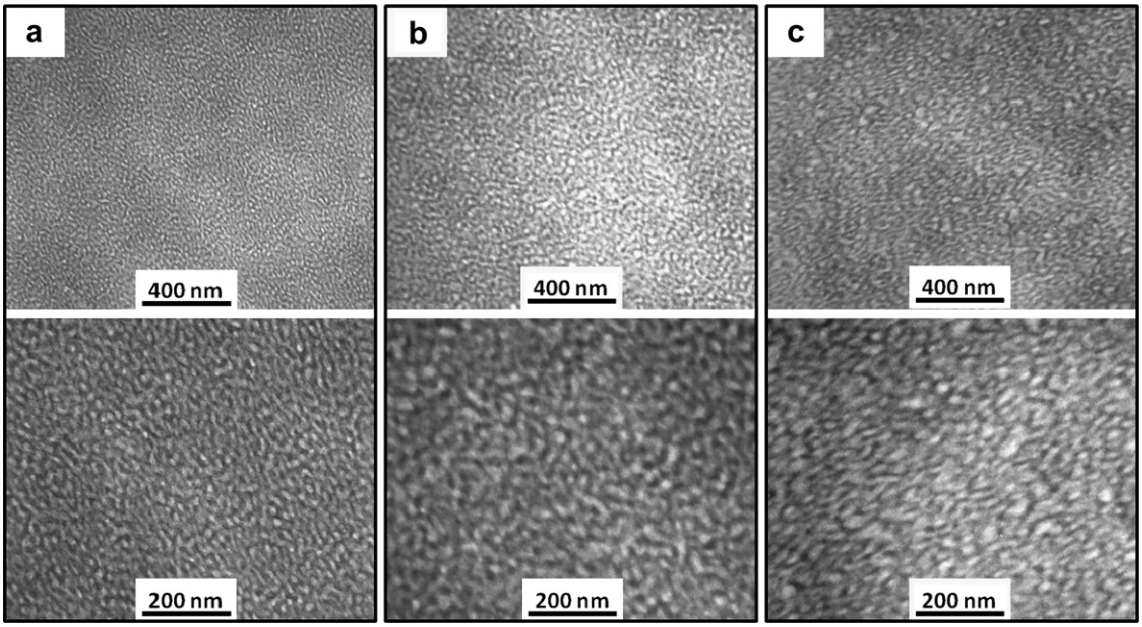

Fig. 1. TEM images of (a) SBS, (b) SBS-PS, and (c) SBS-PS-SBR films with the OsO_4-stained PB phase.

microdomains (the bright area) can be recognized. Therefore, we suggest that the major possibility to form completely dissolution of PS in SBS block copolymer. The morphological transformation can be observed from worm-like structure to network structure when SBS are blended with SBR as shown in Fig. 1c. The incorporation of SBR in the SBS-PS system may force the polystyrene segments, located originally in the interface between PB and PS block, to segregate to the polystyrene phase. It is reasonable to infer that the compatibilization is the results of entropic origin. The influence of the additives on the SBS star-block copolymer viscoelastic properties was investigated by preparing a series of additives/SBS blends. Fig. 2 plots E′ as function of temperature for the pure star-block copolymer and its blends. The result shows that there are significant reductions in E′ across the plateau region in a pure star-block copolymer (33 wt % oil content). Therefore, we suggest that oil acts as plasticizer above melting temperature. The storage modulus of the blends is much higher that of the pure star-block copolymer from −40 °C to 40 °C investigated. The mechanical properties change suggests that the miscibility between the blend is not good. The moduli of the modified systems improve 1-fold as compared to the neat systems to increased molecular entanglements. For pure SBS, two T_{gs} at −86 and 76 °C, are observed one can be assigned to the T_g of PB and the T_g of the PS, respectively. There is a little shift in the T_g of PB segment as the PS added. This means that the addition of PS leads to a significant change in the phase interaction of the SBS star-like copolymer. It is observed that calcium carbonate compounding provides enhanced stiffness to the SBS star copolymer. Moreover, the incorporation of SBR in the SBS-PS can transform morphological from worm-like structure to network structure. As observed, the network microstructure is available for bubble growth, this leads to larger cells and lower foam density [14].

The additions of PS and SBR in SBS could increase the size of PS domains and the strength of the boundary between PS and PB domains as shown in Scheme 1a. In addition to the blowing agent AC and the crosslinking agent DCP, the silicon dioxide (SiO_2) nanoparticles are also important trace additives for the heterogeneous growth of separated microballoons from these fine particles [11]. Others such as pentaerythritol tertkis(3,5-di-*tert*-butyl-4-hydroxyhydrocinnamte) (PT) and white oil are used as antioxidant, processing oil. DCP and AC are the common crosslinking and blowing agents of saturated or unsaturated polyolefins, respectively. DCP has a half-life of 10 h at 115 °C and 1 min at 171 °C [2b,15], and for chemically blown polyethylene, polyvinylchloride,

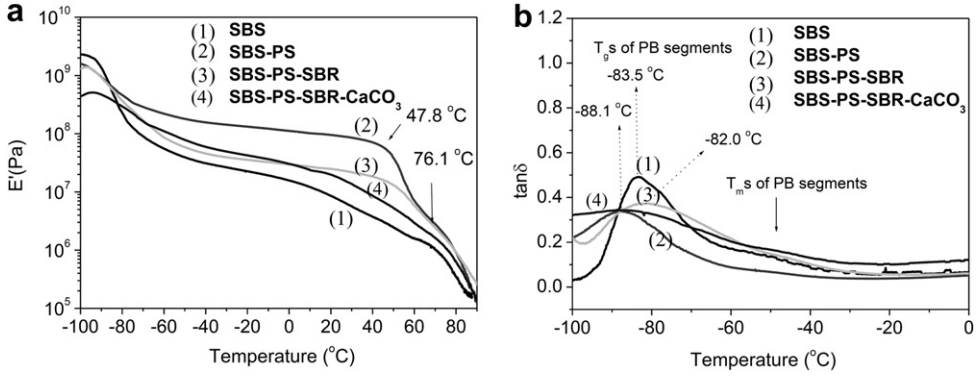

Fig. 2. Storage modulus responses and tan δ response from polymer blends at temperatures from −110 to 100 °C.

Table 2
Physical and mechanical properties.

Samples	Cell Size	Density[a]	Hardness[b]	Shrinkage[c]	Strength		Elongation[f]	CS[g]	VT[h]
					Tensile[d]	Tear[e]			
	(μm)	(g/cm^3)	(shore C)	(%)	(kg/cm^2)	(kg/cm)	(%)	(%)	(min)
I	28.5 ± 17.6	0.91	72	0	30.89	15.44	551	67	40
II	78.8 ± 30.5	0.14	15	4.0	7.0	2.6	350	88	9.2
III	65.1 ± 38.0	0.16	16	4.5	6.5	2.4	325	80	9.3
IV	57.0 ± 30.3	0.20	23	5.0	9.2	3.2	270	77	10.4
V	45.2 ± 23.2	0.21	26	5.0	10.2	3.8	233	73	10.2
VI	35.9 ± 20.8	0.24	32	7.5	10.0	3.7	198	65	11.1

[a] Tested by ASTM D792.
[b] Tested by ASTM D2240.
[c] Applied by ASTM D1204.
[d] Applied by ASTM D412-C.
[e] Applied by ASTM D624-C.
[f] Applied by ASTM D412.
[g] Compression Set is tested by ASTM D-395
[h] Vulcaization Time (t90).

or PS foams, the yellow-orange powders of AC is usually set to decompose at 195 °C because of the wide-range decomposition from 160 to 210 °C for the different particle size [16]. The different decomposition temperatures of DCP and AC allow the crosslinking reaction prior to the foaming process.

3.2. Microstructures

Values of the average cell size were determined as a representative parameter of the foam microstructure (Table 2). The final cell micrographs of the foams are shown in Fig. 1 under study. From this figure and the data of the cited tables, several interesting results can be inferred about the cellular structure of each type of materials. Foams produced from the decomposition of AC are isotropic, small and polyhedral-shaped (Fig. 3a). High magnificent micrographs (Fig. 3b) also show that partial cell walls with the thickness of about 10 μm can improve the mechanical strength of polymer scaffolds. This kind of structure is expected taking into account that no physical blowing agents are used in these materials and that foaming is carried out in an isotropic way, without any preferential direction of process or physical constraints. It is seen that sample I shows a very small numbers of cells which is nearly nonfoamed. With the increasing of DCP content 0.1–0.2 phr, it is observed that number of cells are increased and cells are created finer in size (Table 2). With the smaller average size of the cell of 35.9 ± 20.8 μm for Sample VI, the distribution of cells in the SBS/PS/

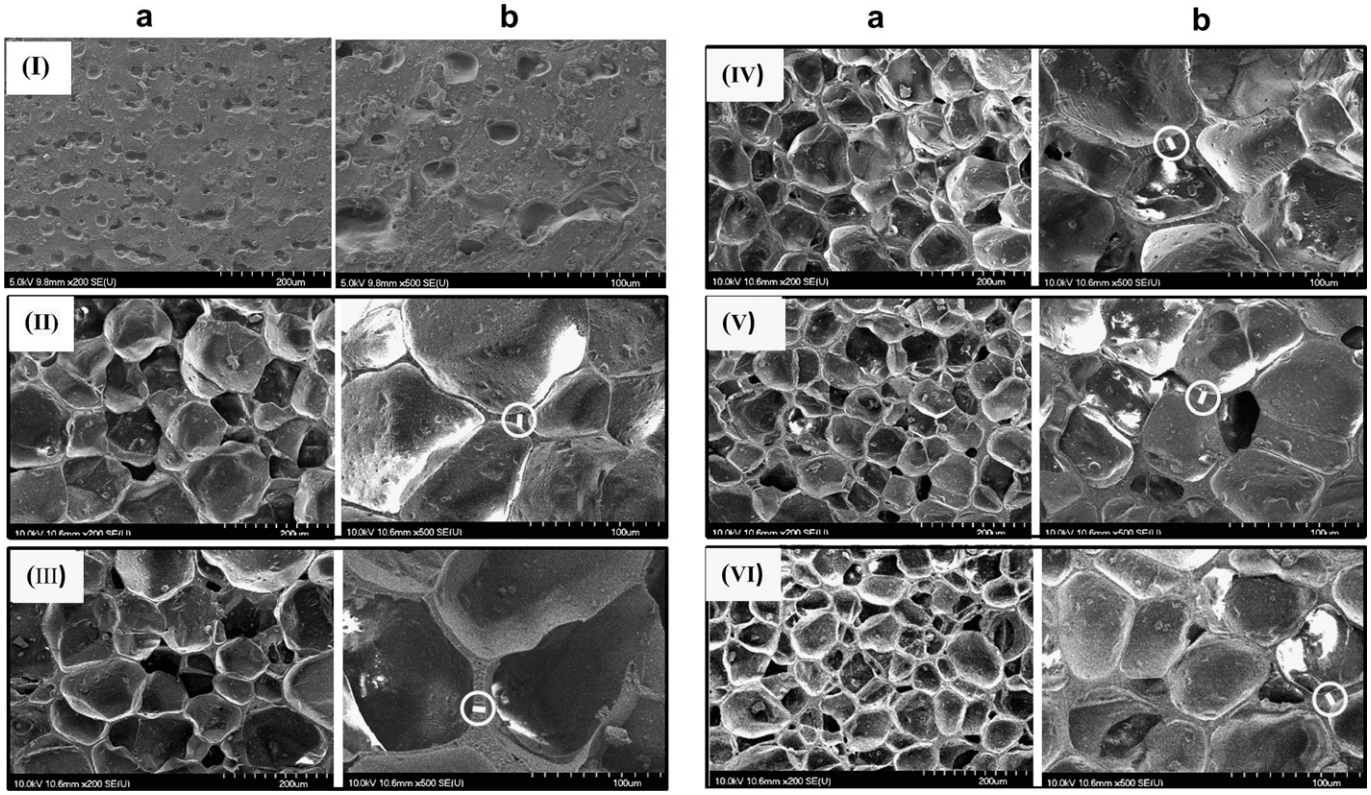

Fig. 3. SEM images of (a) surface regions and (b) internal regions at 200× and 500× magnification for samples I–VI. White spots are indicative of electron charge and white bars within a white cycle are 10 μm in length.

SBR foam would be denser, resulting in the higher density of 0.24 g/cm^3. As expected, in the presence of DCP, the partial ethylene group of PB chains could link together and form a chemical network. With increasing the content of crosslinking agent, the melting strength and the viscosity of SBS/PS/SBR blends at 160 °C would be strong enough to prevent from the diffusion and the combination of gas bubbles which is produced from the decomposition of AC. The blowing agent AC and the crosslinker of DCP were adjusted to get the same degree of foam density. Due to the foaming route a homogeneous cellular structure along foam block thickness has been observed by the SEM image on the surface and in the interior of SBS/PS/SBR foams (Fig. 3a and b). It is clearly observed that DCP agent plays a positive role with the refinement (cell size, shape and distribution) of microcellular structure compared to without crosslinker. The foam structural variability is likely to affect its mechanical properties. In the following discussion, we can observe the different properties with the effect of crosslinking agent.

The physical and mechanical properties of samples I–VI are listed in Table 2 [17]. No DCP composition shows higher values compared to crosslinking samples. With the crosslinking agent DCP from 0.1 to 0.2 phr, the density of SBS/PS/SBR foams would increase from 0.14 to 0.24 g/cm^3 due to the low expansion of the slightly crosslinked PB. Polymer crystallinity and degree of crosslinking have a significant effect on hardness of microcellular foams. For a material at a given degree of crosslinking, foam density also has a significant effect on hardness; the lower the density the softer the foam (see the hardness and the density of Samples I–VI in Table 2). However, there is usually a tradeoff between the positive attributes of lower foam density (softer, more comfortable foam at lower weight) and the positive attributes of compression set (rebound resilience, split tear, and heat shrinkage). A common approach used to optimize the combination of desirable features is to use a separate sock liner or insole close to the foot and a midsole underneath. The insole at low foam density (0.1–0.2 g/cm^3) provides maximum softness, while the midsole at higher foam density (0.18–0.35 g/cm^3) provides the high resilience, low compression set, high split tear, and low shrinkage. Table 2 shows that the cell density increased as the DCP increased, as expected. As a consequence, a higher cell population density is developed in the SBS/PS/SBR crosslinking foam.

The tensile strength of microcelluar foams without crosslinking is directly proportional to the foam density, which is simply controlled by the concentration of the blowing agent. Herein, with be involved in the crosslinking, the strength of microcellular SBS/PS/SBR foams increases more with the increase of the content of DCP. This is because the chemical linkages between PB chains would improve the resistance to the deformation (the displacement between chains) under the external force. While applying a load, the elongation of polymer rubbers is based on the extension

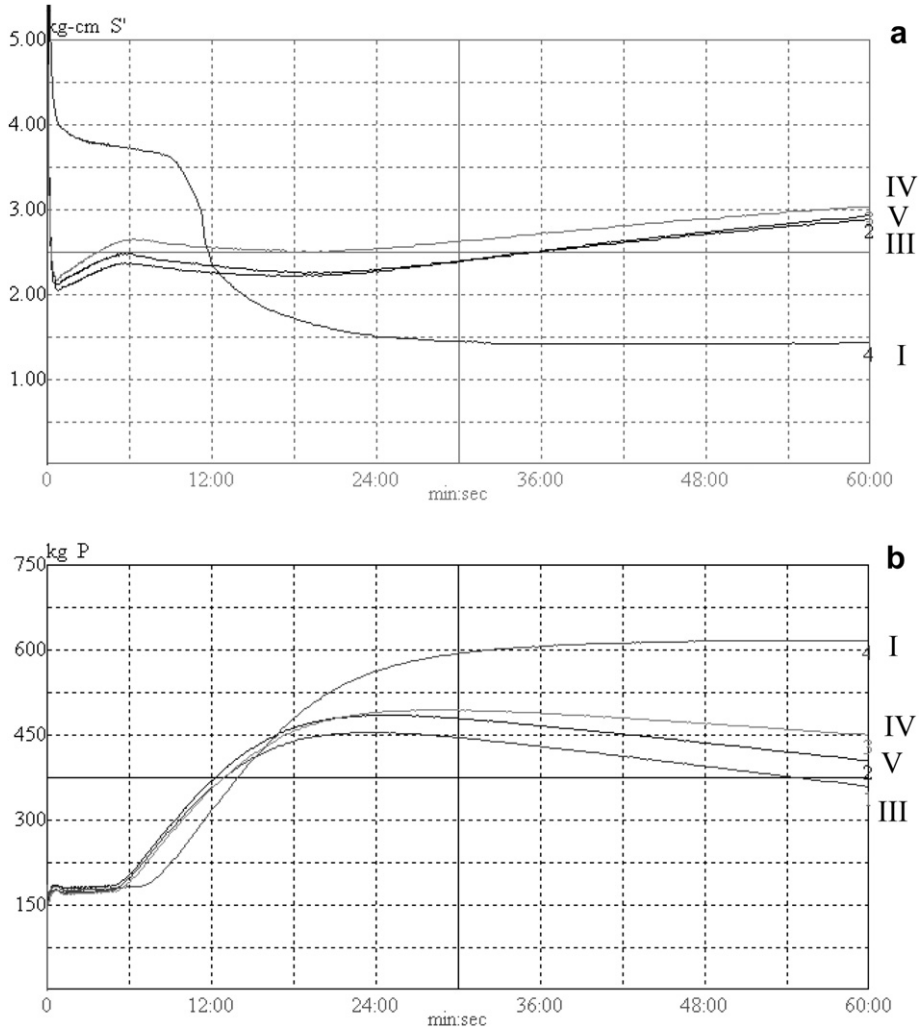

Fig. 4. Rheographs and blowing curves of SBS/PS/SBR blend at 160 °C.

of soft chains. With similar reasons to the tensile strength, the tensile elongation at break reduced with increasing the concentration of DCP because each crosslinking point would be a gel position which divides PB chains into smaller segments. High split tear relates to durability of the foam; that is, strength over the long term as well as the short term. As in the case of compression set, high split tear typically requires high foam density, and high degree of crosslinking (see the density and the tear strength of Samples I–VI in Table 2).

The compression set test measures permanent set of the foam, the lower the permanent set the better the elastic recovery of the foam. Low compression set is desirable to maintain cushioning for long term use, which in turn relates to durability with respect to comfort and rebound resilience. Low 50 °C compression set usually requires high foam density, and high degree of crosslinking, cf. the density and crosslinking effect on Samples II–VI in Table 2; however, high foam density negatively impacts the highly desirable trait of low weight, and high polymer crystallinity gives harder foams with low rebound resilience. Table 2 summarizes the t90 values, the period time to reach 90% maximum torque, of the crosslinked SBS/PS/SBR blends [18]. It can be seen from Table 2 that the incorporation of DCP has increased the value of VT. From theory [19], it is known that the torque difference showed shear dynamic modulus which indirectly related to the crosslink density of the compounds. Hence, it can be concluded that the increase of VT has contributed to the better crosslinking while adding more DCP. A typical MDR rheograph for the SBS/PS/SBR blend system is shown in Fig. 4. In both cases, S′ increases and foam pressure increases as the curing of the rubber progress. At a very short time (generally less than 2 min), however, there occurs a decrease in S′. This is due to the initial heat softening of the rubber compound. Therefore, the relationship between the vulcanization rate and blowing agent decomposition can be improved by the addition of crosslinking agent of DCP.

3.3. Thermal properties

The TGA curve of pristine SBS, SBR, and PS at a heating rate of 20 °C/min indicates the single stage of SBS starts decomposing around 400 °C and ends at about 500 °C [20]. However, the TGA curves of Samples I–VI (see Fig. 5 and Table 3) show three-step decompositions with these observations: the average onset points at 200, 417.0, 667.6 °C and the average weight loss of 23.3, 48.7 and 11.3 wt % for Stages A, B, and C, respectively. The first thermal decomposition temperature (150–340 °C) comes from the boiling of oil results in the loss of 23.3 wt % (~86.4 × 33 wt %). After

Table 3
Results of TGA thermograms.

Samples	Stage A		Stage B		Stage C		Residue
	OP[a]	WL[b]	OP	WL	OP	WL	at 750 °C
	(°C)	(wt %)	(°C)	(wt %)	(°C)	(wt %)	(wt %)
I	194.4	25.4	423.8	49.3	644.0	10.5	15.3
II	187.7	24.2	421.9	49.3	666.8	11.0	15.1
III	197.2	23.0	417.1	46.6	664.9	13.0	15.0
IV	197.2	23.7	411.3	48.7	669.8	10.7	15.0
V	197.4	23.2	416.9	50.1	666.2	11.5	14.8
VI	196.3	23.6	414.1	49.1	670.5	11.3	14.8
Average	195.0	23.8	417.5	48.8	663.7	11.3	15.0

[a] Onset point.
[b] Weight loss.

decomposition of the oil, the blends containing SBS, SBR, and PS is stable up 500 °C, which is identical to the decomposition temperature of the above mentioned literatures. When the temperature reached 500 °C, the decomposition of $CaCO_3$ started and till 740 °C the mass weight constant. Here, the $CaCO_3$ was decomposed to CaO and CO_2. Therefore, Samples I–VI show the average residue yield of 15.0 wt % at 750 °C.

The T_g of the SBS/PS/SBR foam is especially important, depending on its usage, as in normal applications like a cushion it needs to be in its rubbery state to provide the desired characteristics. The DSC thermograms are not suitable for the investigation of T_g for microcellular polymers due to many insulating cavities in the matrix. For evaluation of thermal endurance in foamed plastics, temperature and time dependence of compression dynamic modulus of SBS/PS/SBR foams was investigated by dynamic viscoelastic measurements. Fig. 6 shows the tan δ (E″/E′) response from the Samples II to VI. The rheological behavior in terms of storage modulus, tan δ of the sample I is similar to neat systems. The intensity and position of the glass transition were dependent on the DCP content in these blends. In view of Samples II–VI, the T_g position shifts from −71.1 to −58 °C (the T_g of −86.7 °C for bulk SBS), showing the restriction of PB molecular motion by increasing DCP crosslinking agent. The transition at −15.4 °C might be the melting transition of short-ranging PB chains, which is confined within crosslinking points [21]. The tan δ peak temperature was 87 °C for Samples II–VI, which were in accord with the results obtained by Masson et al., who reported that the tan δ peak temperature of hard PS ranged from 55 to 90 °C depending on PS content [22]. The wide temperature range of the rubbery state from −50 °C to 60 °C implies that the crosslinking SBS/PS/SBR

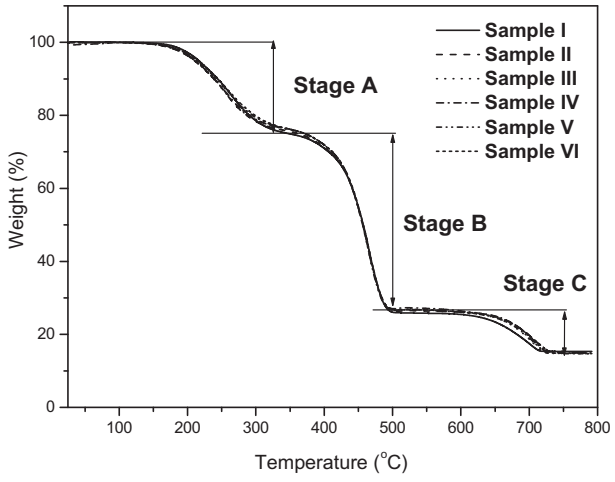

Fig. 5. TGA thermograms of samples I to V.

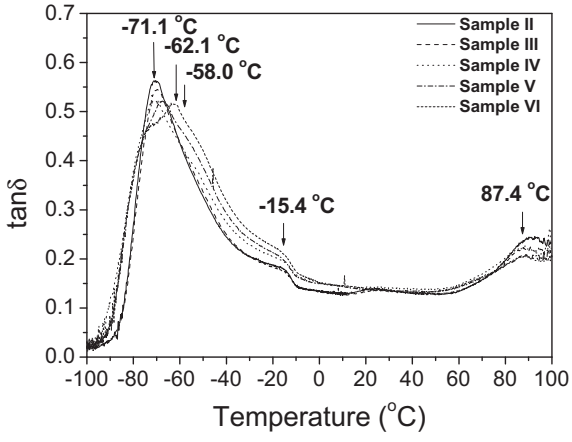

Fig. 6. Tan δ reponse from Samples II to VI at temperatures from −110 to 100 °C.

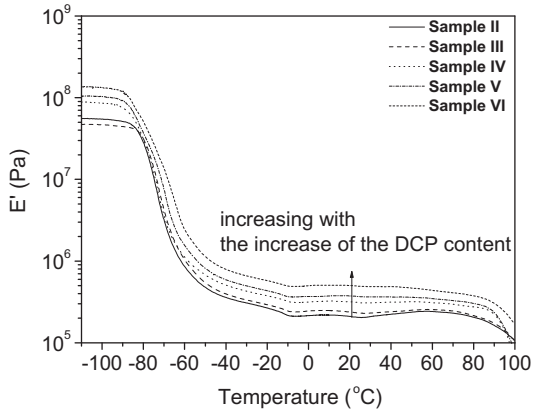

Fig. 7. Storage modulus responses from Samples I to VI at temperatures from −110 to 100 °C.

foams has a great quantity of world-wide cushioning applications from the polar region to the equatorial area.

Fig. 7 shows the storage modulus response from the Samples II to VI. At the fixed concentration of AC, the initial storage modulus at 20 °C increase with increasing the content of DCP. At crosslinker concentrations of 0.18 and 0.2 phr, constant values of 4 and 3.7×10^5 Pa, respectively. This increasing is due to the more crosslinking SBS/PS/SBR cell wall exhibits the stronger elastic properties to recovery its initial dimension after removing the external load. Thus, when the crosslinking condition is appropriate, the crosslinked SBS/SBR samples behave as a normal crosslinked rubber, as expected, even when the PS microdomains no longer act as physical crosslinks. Thus similar results to Fig. 6, the glass transitions of crosslinking soft PB domains and hard PS domains can be observed at around −70 °C and 90 °C. These phenomena indicate that the more content of DCP not only lead to higher storage modulus but also sustain the mechanical response at higher frequency.

4. Conclusions

The concentration of peroxide crosslinker, dicumyl peroxide (DCP), has a great effect on the size distribution of hollow cells and the results of mechanical properties. The SEM images of cross-section of PS/PB foams show the smaller and denser of cell distribution for Sample VI with the 0.2 phr of DCP in comparison with Samples I–V with the same content of blowing agent, azodicarbonamide (AC). With the increase of the DCP concentration, the density, the hardness, shrinkage, tensile strength, tear strength, and vulcaization time increase due to the slightly crosslinking of soft PB domains. The confinement of PB chain motion within crosslinking points retards the elongation at break and reduces the compression set. In addition, the results of dynamical mechanical analyses show the shift of glass transition temperature from −71.1 to −62.1 °C and the increase of initial storage modulus and storage modulus at 20 °C for the increase of the DCP concentration. Moreover, the more content of DCP not only lead to higher storage modulus but also sustain the mechanical response at higher frequency.

References

[1] Gibson LJ, Ashby MF. Celluar solids: structure and properties. 2nd ed. Oxford: Pergamon Press; 1988.
[2] (a) Saint-Michel F, Chazeau L, Cavaille JY, Chabert E. Compos Sci Technol 2006;66:2700;
(b) Dubois R, Karande S, Wright DP, Martinez FJ. Cell Plast 2002;38:149;
(c) Herrington R, Hock K, editors. Flexible polyurethane foams. 2nd ed. Midland: Dow Chemical Co.; 1997.
[3] (a) Hilyard NC, Cunningham A. Low density cellular plastics: physical basis of behavior. London: Chapman and Hall; 1994;
(b) Rodriguez-Perez MA. Adv Polym Sci 2005;184:97;
(c) Klempner D, Frish KC. Handbook of polymeric foams and foam technology. New York: Oxford University Press; 1991.
[4] (a) Holden G. Undertanding thermoplastic elastomers. Munich: Carl Hanser Verlag; 2000. pp. 15–35;
(b) Bates FS, Fredrickson GH. Annu Rev Phys Chem 1990;41:525;
(c) Leibler L. Macromolecules 1980;13:1602;
(d) Honeker CC, Thomas EL. Chem Mater 1996;8:1702;
(e) Pakula T, Saijo K, Kawai H, Hashimoto T. Macromolecules 1985;18:1294;
(f) Harada T, Bates FS, Lodge TP. Macromolecules 2003;36:5440.
[5] Colton JS. The nucleation of microcellular thermoplastic foam. Massachusetts: MIT; 1985.
[6] Jacob S. US Patent 7,319,121 B2; 2008.
[7] Gul RME. Eur Polym J 1999;35:2001.
[8] (a) Chaudhary BI, Barry RP, Tusim MH. J Cell Plat 2000;36:397;
(b) Chaudhary BI, Barry RP. J Cell Plat 1999;35:531.
[9] Jouenne S, Gonzaćlez-Lećon JA, Ruzette AV, Lodećfier P, Leibler L. Macromolecules 2008;41:9823.
[10] (a) Ruckdaschel H, Altstadt V, Muller AHE. Cell Polym 2007;26:367.
[11] (a) Cha SW, Yoon JD, Uto N. Cell Polym 2004;23:229;
(b) Ramesh NS, Lee ST. Cell Polym 2005;24:269;
(c) Caprioli G, Bernasconi R, Hamilton A, Liefferinge MV, Barettini S, Cappella A. J Cell Plast 1999;35:27;
(d) Park CB, Cheung LK, Song SW. Cell Polym 1998;17:221.
[12] (a) Martínez-Díez JA, Rodríguez-Pérez MA, De Saja JA. J Cell Plat 2001;37:21;
(b) Sims GLA, Khunniteekool C. Cell Polym 1996;15:1;
(c) Khunniteekool C. Cell Polym 1996;15:14.
[13] Tonkel RF, Gross AL. US Patent 4,894,933; 1990.
[14] McKay KW, Gros WA, Diehl CF. J Appl Polym Sci 1995;56:947.
[15] (a) Sims GLA, Sipaut CS. Cell Polym 2001;20:255;
(b) Sipaut CS, Sims GLA, Ariff ZM. Cell Polym 2008;27:11;
(c) Sipaut CS, Sims GLA, Mohamad Ibrahim MN. Cell Polym 2008;27:67;
(d) Rodríguez-Pérez MA, Almanza O, Ruiz-Herrero JL, de Saja JA. Cell Polym 2008;27:179;
(e) Mahapatron A, Mills NJ, Sims GLA. Cell Polym 1998;17:252;
(f) Sombatsompop N. Cell Polym 1998;17:63.
[16] (a) Zhou Q, Weiping G, Wu J, Wang J, Zhen HY, Wu Q. J Cell Plast 2000;36:126;
(b) Jaafar HAS, Sims GLA. Cell Polym 1993;12:303;
(c) Sims GLA, Sirithongtaworn W. Cell Polym 1997;16:271;
(d) Zhou Q, Cong CB. J Cell Plast 2005;41:225;
(e) Pop-Iliev R, Park CB, Fenton RG. J Cell Plast 2005;41:519.
[17] (a) Bureau MN, Gendron R. J Cell Plast 2003;39:353;
(b) Bureau MN, Champagne MF, Gendron R. J Cell Plast 2005;41:73.
[18] Ismail H, Chia HH. Eur Polym J 1998;34:1857.
[19] Ismail H, Freakley PK, Sutherland I, Sheng E. Eur Polym J 1995;31:1109.
[20] (a) Lu L, Yu H, Wang S, Zhang Y. J Appl Polym Sci 2009;112:524;
(b) Kwon E, Castaldi MJ. Environ Sci Technol 2009;43:5996;
(c) Bourbigot S, Gilman JW, Wilkie CA. Polym Deg Stab 2004;84:483.
[21] Brozek J, Budin J, Roda J. Therm Anal Calorim 2007;89:211.
[22] Masson JF, Bundalo-Perc S, Delgado A. J Polym Sci Part A Polym Phys 2005;43:276.